XMM-Newton Calibration Technical Note

XMM-CCF-REL-389

XMM-Newton EPIC-pn: long-term CTI update

Ivan Valtchanov, Michael Smith

March 31, 2022

1 CCF components

Name of CCF	VALDATE	EVALDATE	Blocks changed	CAL version	XSCS flag
EPN_CTI_0055.CCF	2000-01-01T00:00:00		LONG_TERM_CTI COMB_EVT_OFFSET	3.240	NO
EPN_CTI_0056.CCF	2000-03-23T05:00:00		LONG_TERM_CTI COMB_EVT_OFFSET	3.240	NO

2 Changes

To date, the empirical EPIC-pn long-term charge-transfer inefficiency correction (LTCTI) for Full Frame (FF) and Extended Full Frame modes (EFF) is derived using the Al Kα (1.486 keV) and Mn Kα (5.8988 keV) emission lines, which are produced by the radioactive Fe-55 source in *CalClosed* exposures.

The main change contained in this release is the inclusion of an additional reference energy for the LTCTI, at 8.038 keV, derived using the fluorescent Cu Kα line, using all suitable pn observations in FF and EFF modes. Epoch-independent offsets for double events (patterns from 1 to 4) are also calculated and incorporated in the calibration table. This is described in Section 3.

In addition, this release contains the periodic update of the LTCTI modelling derived at Al Kα and Mn Kα energies (see Section 4).

3 LTCTI at 8 keV using copper fluorescent line

In deriving the LTCTI correction we use the same functional model as in Smith et al. (2010), i.e.:

$$E_{\rm corr} = E \times \left(\frac{1-a}{1-{\rm TCOEF}(t)} \right)^{RAWY}, \quad (1)$$

where $E_{\rm corr}$ is the long-term CTI corrected energy for an event with energy E at RAWY coordinate[1]. TCOEF(t) is a suitable function depending on epoch and CCD number, and a is a normalisation constant, by design $a = {\rm TCOEF}(t = 0)$. The function TCOEF is derived at each reference energy, which in this case is that of the copper fluorescent line Cu Kα at 8.038 keV. The values are tabulated on a time grid and stored in the `LONG_TERM_CTI` extension.

At validation, however, we observed a time-dependent systematic offset in the corrected energy of the line. Hence, we implemented a two-step procedure to correct for this systematic deviation. More details on this two-step approach are provided in Valtchanov (2022).

The LTCTI is optimised for the full area of the non-central pn CCDs (CCDNR in 2, 3, 5, 6, 8, 9, 11 and 12) and for a smaller area for the central ones (CCDNR in 1, 4, 7 and 10), see e.g. the upper right panel in Fig. 36 of the the XMM-Newton Handbook, Section 3.3.7.2. A notable difference with the LTCTI for the Iron-55 lines is that we do not have copper emission around the boresight, so we can only optimise the LTCTI at RAWY $\leq$ 100-120, for the central CCDs.

Once we have the LTCTI for single events (pattern = 0), we reprocess all FF and EFF observations and calculate the energy offsets of the best fit line centroid for double events, for each of the four patterns. These offset values, as with the Al Kα and Mn Kα lines, are time-independent, they only depend on CCD number and mode.

The results for single events, in terms of the difference of the best-fit Cu Kα centroid after the correction and the expected energy of the Cu Kα line (8038 eV), are shown in Appendix A.

The overall average residuals and their st.dev. for single and double events for FF and EFF are shown in Fig. 1.

4 Update of the long-term CTI corrections

The parameters which describe the LTCTI correction are routinely updated whenever newly accumulated calibration data deviates significantly from the model extrapolations. *CalClosed* observations are regularly taken in FF and EFF modes, and for these modes the respective LTCTI parameters can be directly derived (see Smith et al. 2014). However, the extended nature of the

[1]The event energy E is corrected for gain (including due to quiescent background) and time-independent CTI.

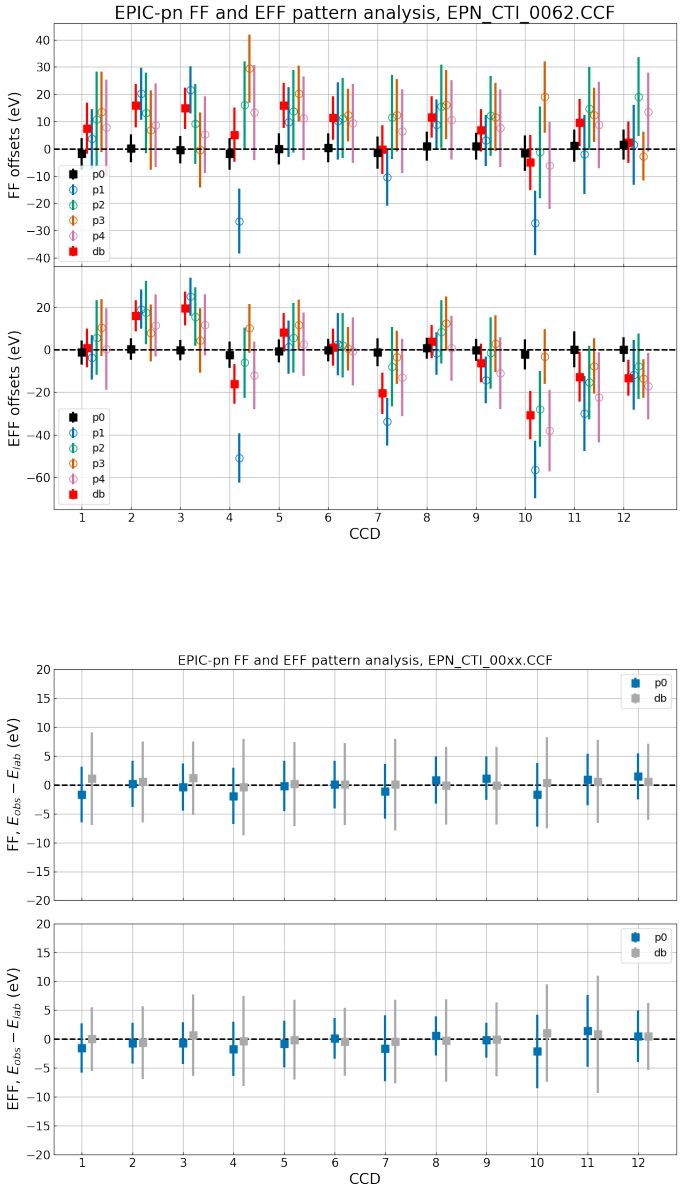

Figure 1: Top: best-fit energy differences for the Cu Kα line for patterns 1 to 4 for FF (upper panel) and EFF (lower panel), time averaged per CCD. The single events (in black, p0) are already corrected for LTCTI, the differences for each pattern from 1 to 4 are incorporated in the `OFFSETS` table in `EPN_CTI_0055/0056.CCF`. Bottom: same as top panel but after correcting the double events for offsets, for clarity we only show the combined double events pattern.

CalClosed emission is less suited for deriving the CTI of the windowed and fast modes, so the LTCTI models used in these cases are partially based on that derived from FF mode (e.g. for Small Window, Timing and Burst modes at both Al Kα and Mn Kα and for Large Window mode at Al Kα; see Valtchanov et al. 2019a,b). Note that, for imaging modes, for CCD 4 the LTCTI correction is optimised for a region around the nominal aim-point (RAWY in 181-200) while for the other CCDs it is optimised for the full (albeit well-illuminated) areas.

This LTCTI update is based on data obtained up to revolution 4042 (January 2022).

4.1 Scientific impact and estimated quality

The new CCF mainly impacts observations taken since $\sim$ 2018, especially FF mode data taken from CCD 1 and at the nominal aim-point in CCD 4. Compared with the previous calibration the CCF yields improvements in energy scale reconstruction of up $\sim$ 20 eV at 6 keV.

A comparison of results obtained with the old and new calibration for FF mode data are shown in Figs. 2, 3 and 6, and for EFF mode data in Figs. 4, 5 and 7.

5 Test procedures

Verification of functionality of EPN_CTI_0055.CCF and EPN_CTI_0056.CCF with SAS 20.0: `calview`, `cifbuild`, `epproc`, `epchain`.

6 Future improvements

- We assumed the centroid of the Cu Kα line to be at 8038 eV[2]. Modelling of the copper Kα lines like in Hölzer et al. (1997) and then convolving with the XMM response should provide a better estimate for the line centroid. Our preliminary checks with those models in XSPEC show that the actual centroid for the total Cu Kα is at 8042 eV.
- As the PN LTCTI will continue to develop in time, model parameters will have to be periodically updated. (The Iron-55 source Al Kα and Mn Kα lines and the fluorescent Cu Kα line should be used together to derive the LTCTI correction curves. Note that there is nothing wrong with the current approach as we do not derive the correction at Cu Kα after correcting for LTCTI at Al Kα and Mn Kα. The correction curves at each line are derived from events uncorrected for LTCTI. Combining the three lines, however, will simplify the workflow for future updates to the LTCTI.)

[2]This is based on the weighted average of Cu Kα_1 and Cu Kα_2, as described in this report.

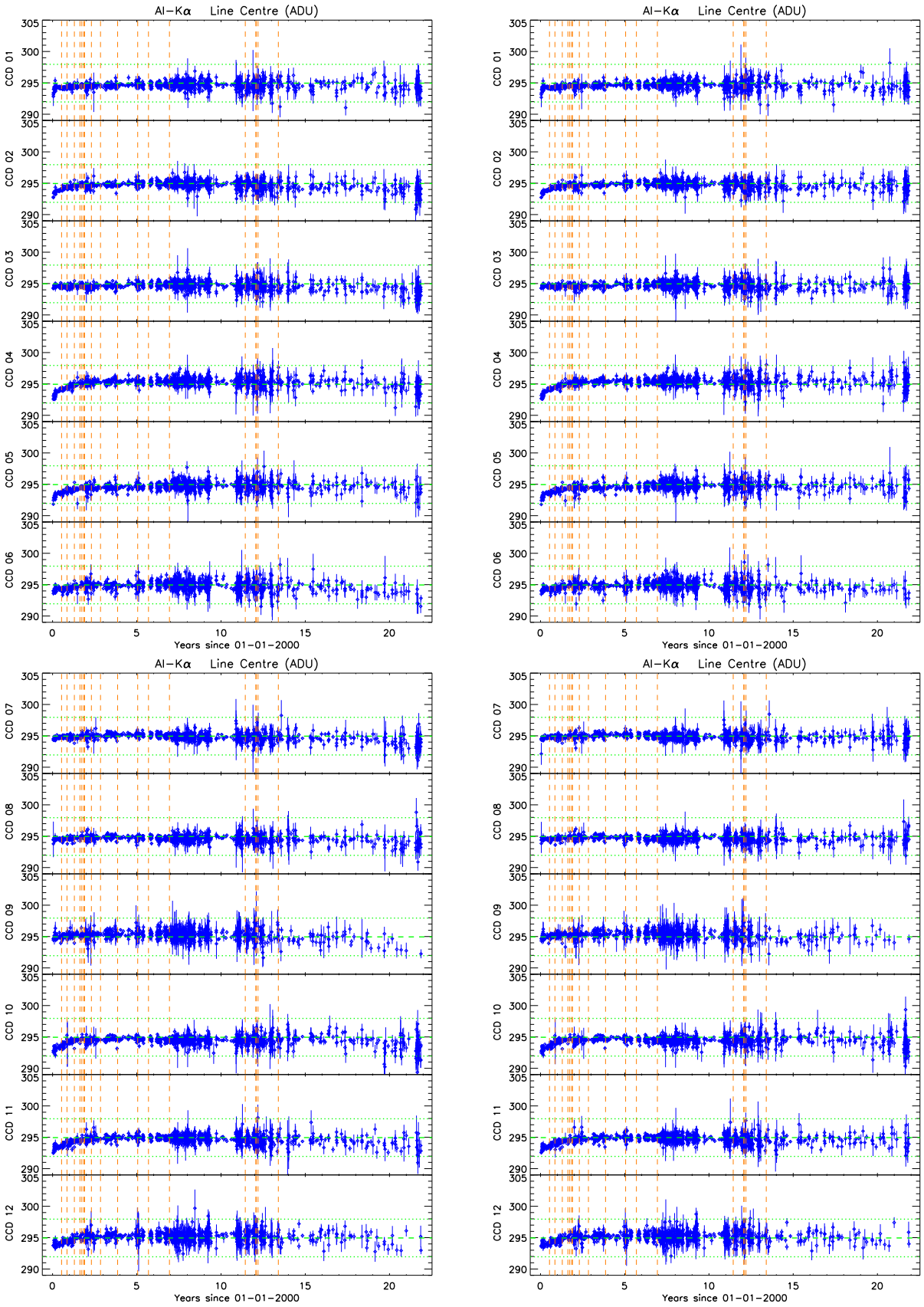

Figure 2: Comparison of the Al Kα reconstructed line centroid energies (in ADU) as determined from FF mode *CalClosed* observations using the old (*left panels*) and new (*right panels*) long-term CTI calibration. The data shown here are based on first-single events extracted from the well illuminated areas of the complete CCDs. The nominal line energy and the ± 3 ADU margin are shown by the green dashed and dotted lines, respectively; the vertical dashed lines indicate the times of major solar coronal mass ejections.

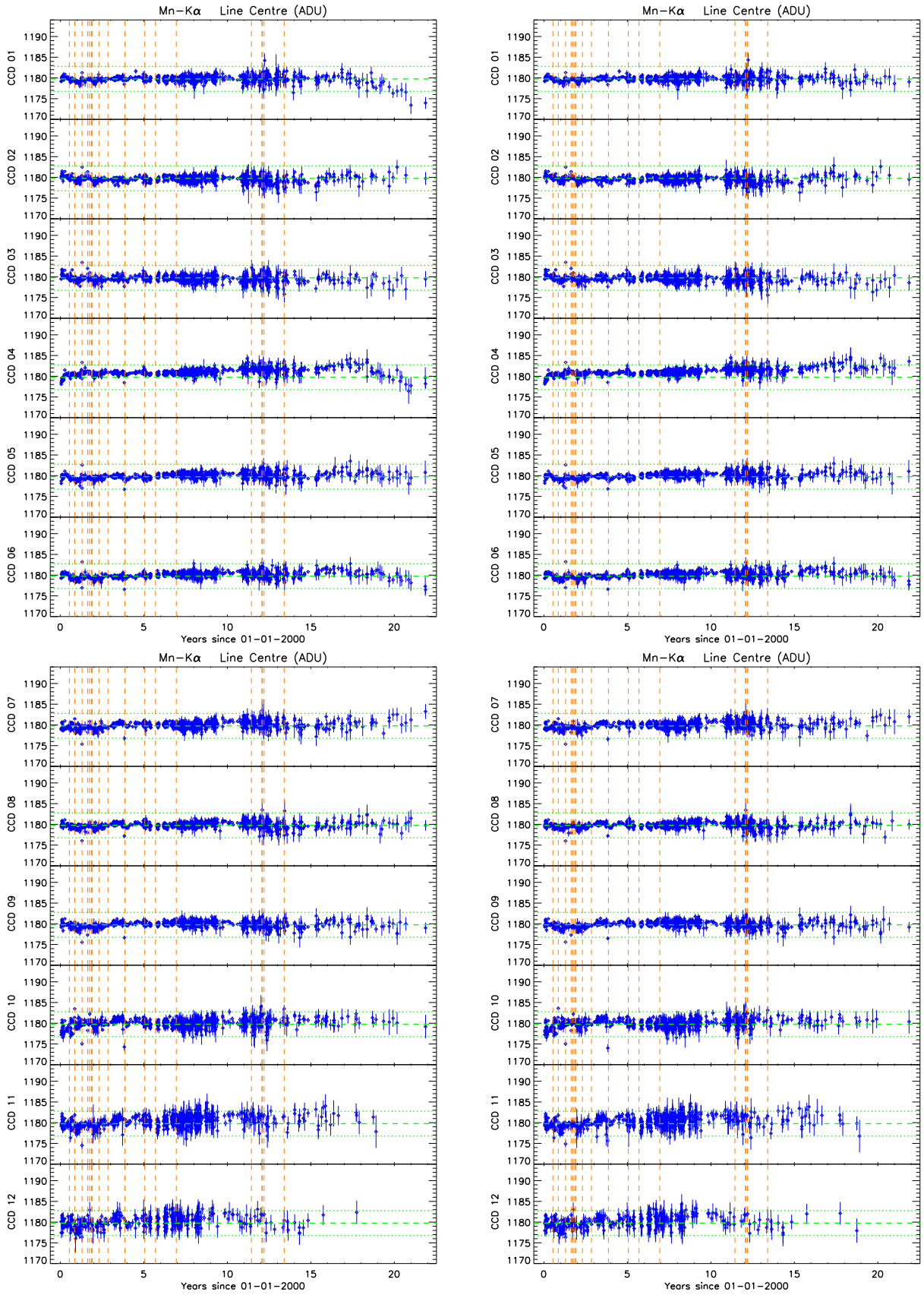

Figure 3: As Fig 2, for FF mode at Mn Kα.

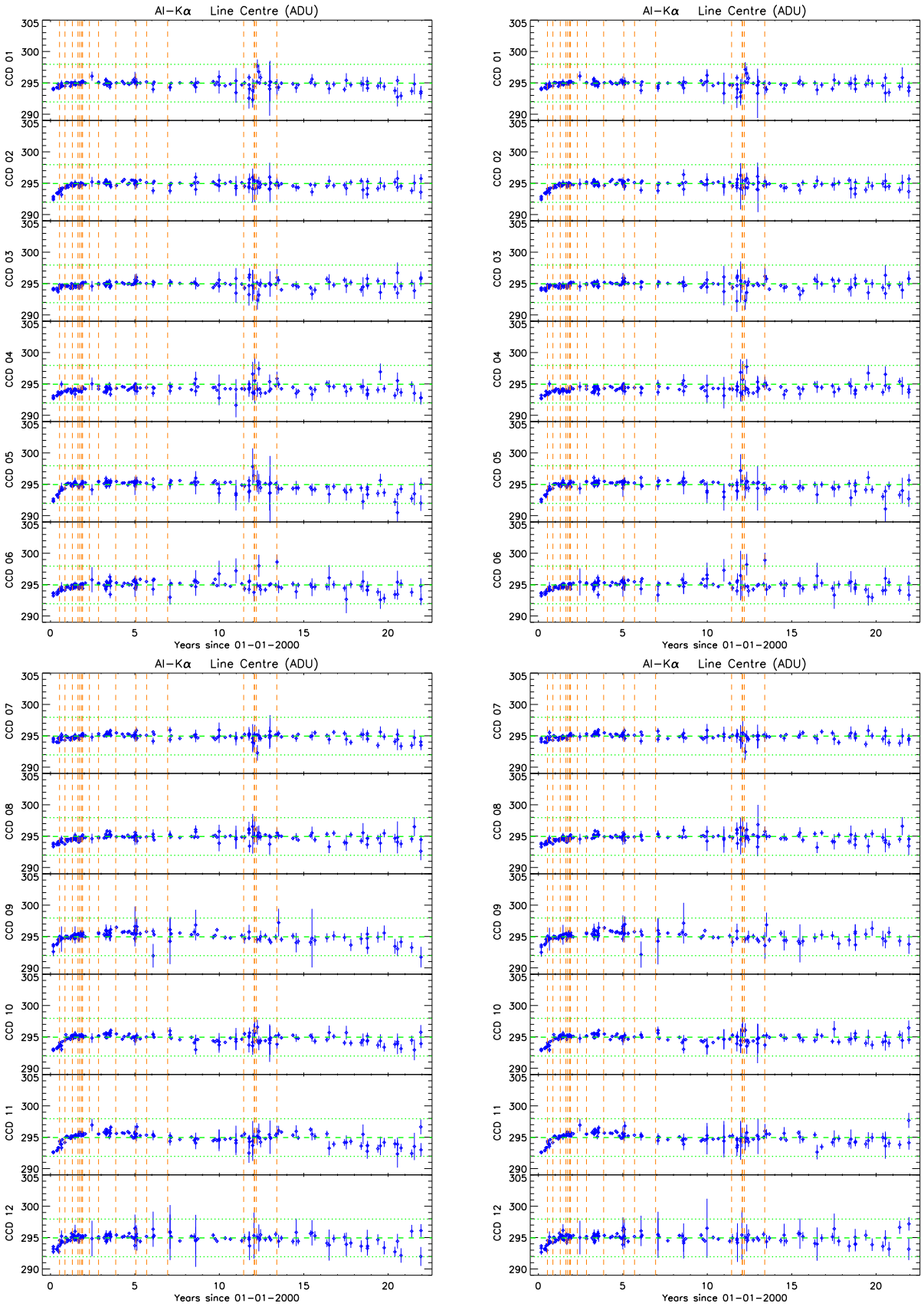

Figure 4: As Fig 2, for EFF mode at Al Kα.

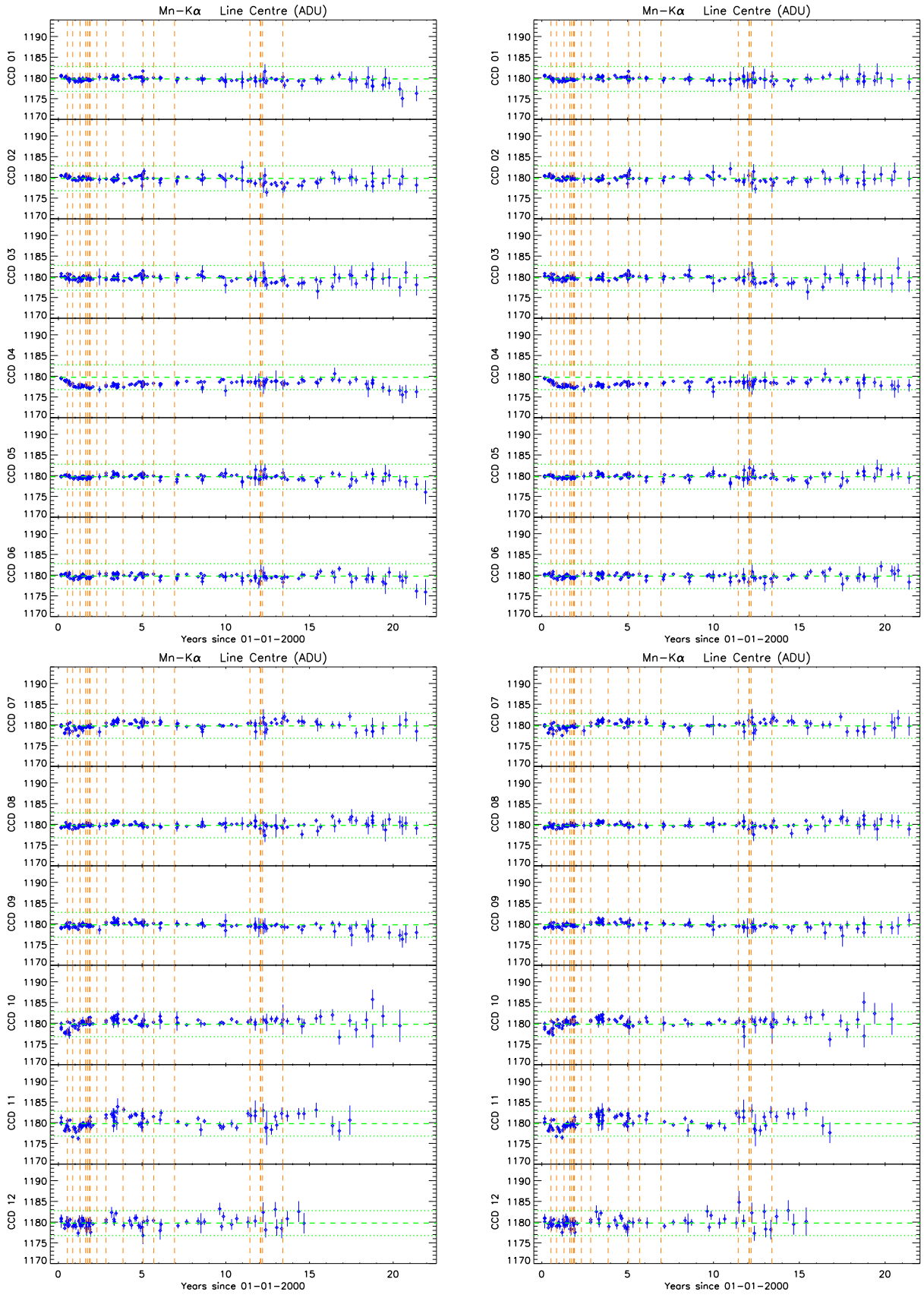

Figure 5: As Fig 4, for EFF mode at Mn Kα.

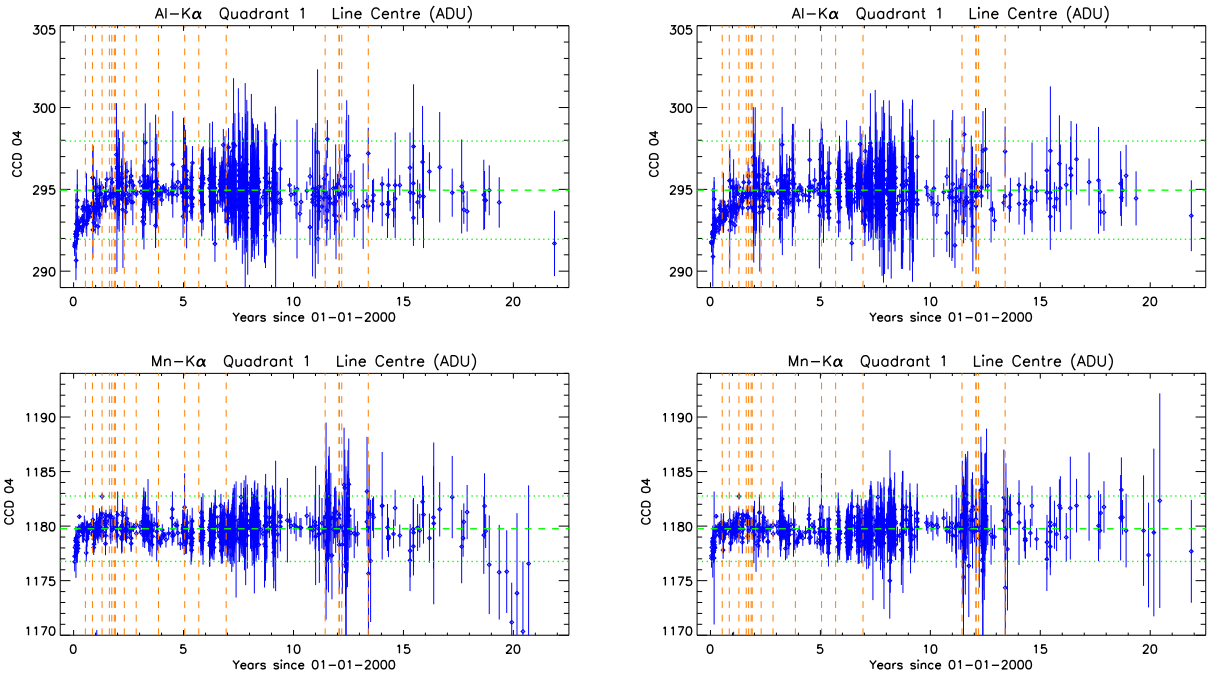

Figure 6: Comparison of reconstructed line centroid energies (in ADU) as determined from FF mode *CalClosed* observations using the old (*left panels*) and new (*right panels*) long-term CTI calibration. Results are shown for Al Kα (top row) and Mn Kα (bottom row). The data shown here are based on first-single events extracted from a 20-row region around the boresight. The nominal line energy and the ± 3 ADU margin are shown by the green dashed and dotted lines, respectively; the vertical dashed lines indicate the times of major solar coronal mass ejections.

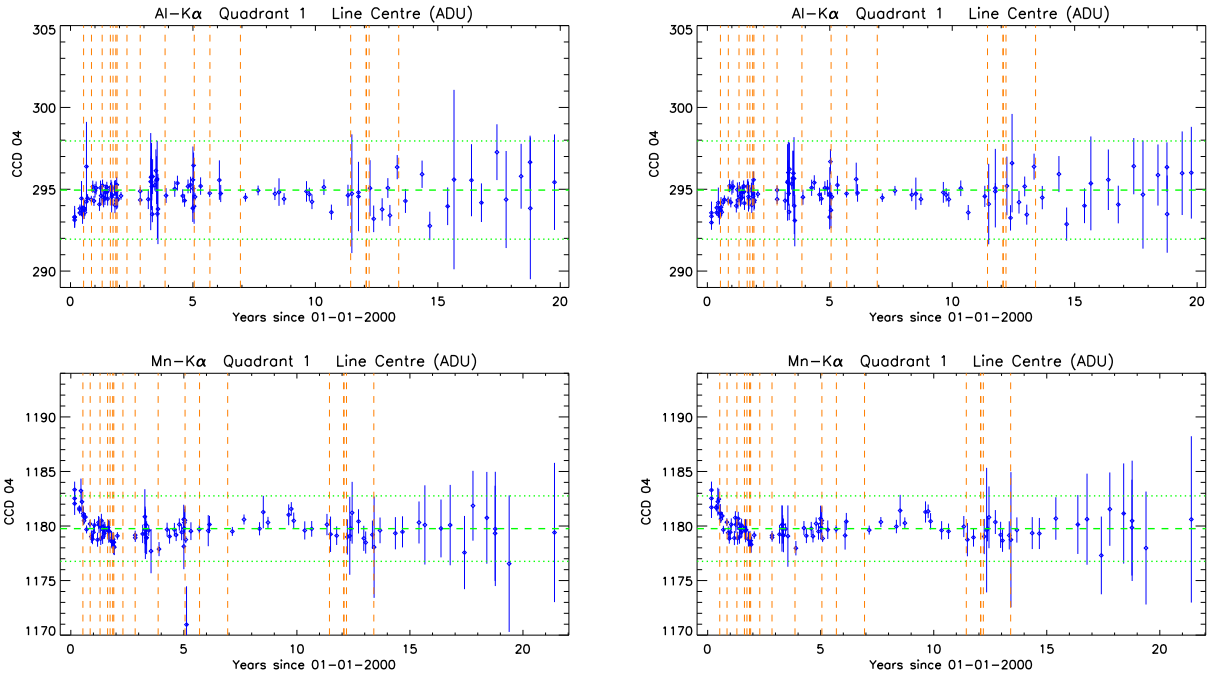

Figure 7: As Fig 6, for EFF mode.

References

Hölzer, G., Fritsch, M., Deutsch, M., Härtwig, J., & Förster, E. 1997, Phys. Rev. A, 56, 4554, doi: 10.1103/PhysRevA.56.4554

Smith, M. J. S., Guainazzi, M., & Cappi, M. 2010, EPIC-pn Long-Term CTI, Tech. Rep. XMM-CCF-REL-271, XMM SOC

Smith, M. J. S., Stuhlinger, M., Saxton, R. D., & Freyberg, M. J. 2014, EPIC-pn Long-Term CTI and Energy Scale, Tech. Rep. XMM-CCF-REL-323, XMM SOC

Valtchanov, I. 2022, XMM-Newton EPIC-pn Energy Scale at 8 keV: two step long-term CTI correction for Full Frame and Extended Full Frame modes, Tech. Rep. XMM-SOC-CAL-TN-231, XMM SOC

Valtchanov, I., Smith, M. J. S., & Schartel, N. 2019a, EPIC-pn Energy Scale for Small Window Mode: long-term CTI correction, Tech. Rep. XMM-CCF-REL-366, XMM SOC

—. 2019b, EPIC-pn Energy Scale for Large Window Mode: long-term CTI and pattern corrections, Tech. Rep. XMM-CCF-REL-367, XMM SOC

A Residuals of Cu Kα line after the two-step correction.

The results in this appendix are after we reprocess the observations with `EPN_CTI_0055.CCF` and `EPN_CTI_0056.CCF`.

A.1 Full Frame mode, single events

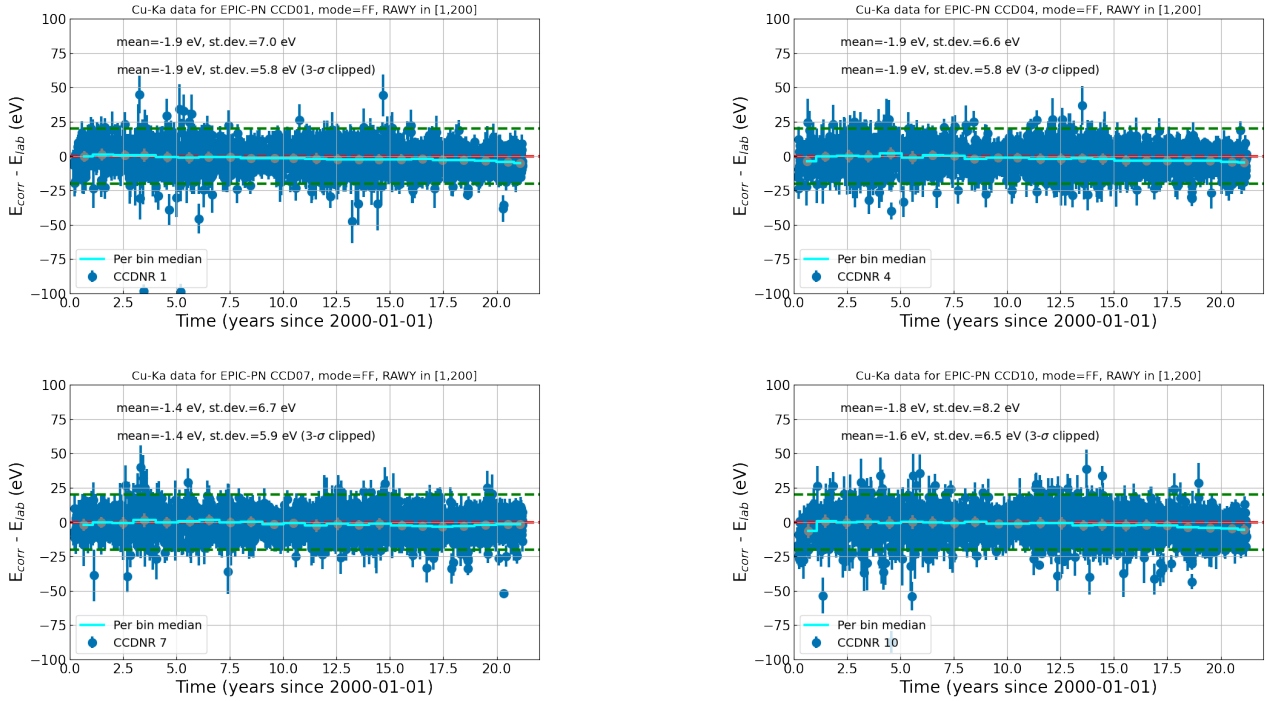

Figure 8: The residual $E_{corr} - E_{lab}$ in eV as function of time for the central CCDs. The red dashed line is zero difference, the two green dashed lines are at ± 20 eV. The cyan steps are the aggregated median values in bins of 500 revolutions. The overall mean and st.dev. and the corresponding 3-σ clipped ones (to discard outliers) are annotated.

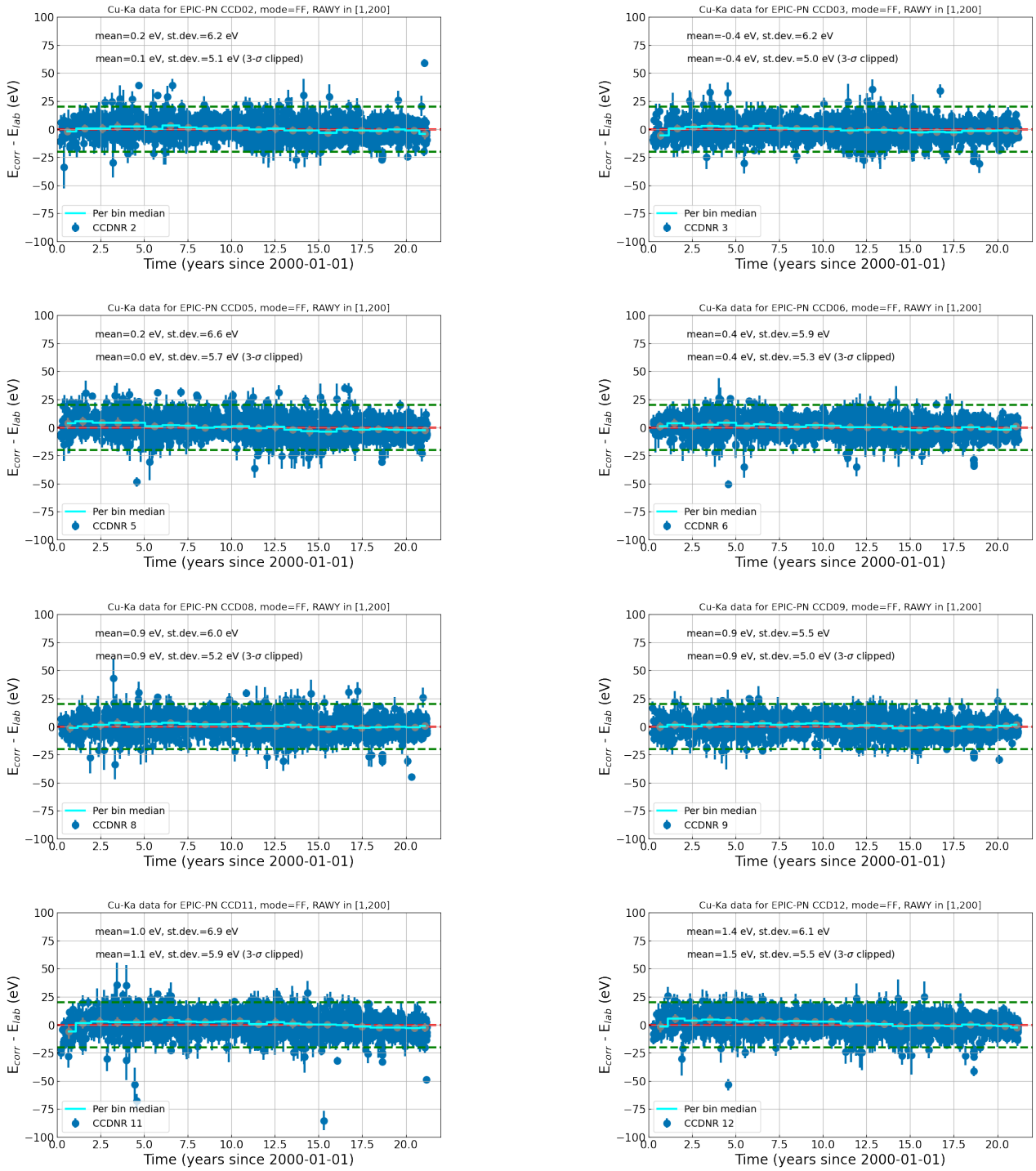

Figure 9: FF residuals after applying the second pass LTCTI for the non-central CCDs. See caption of Fig. 8 for details.

A.2 Extended Full Frame mode, single events

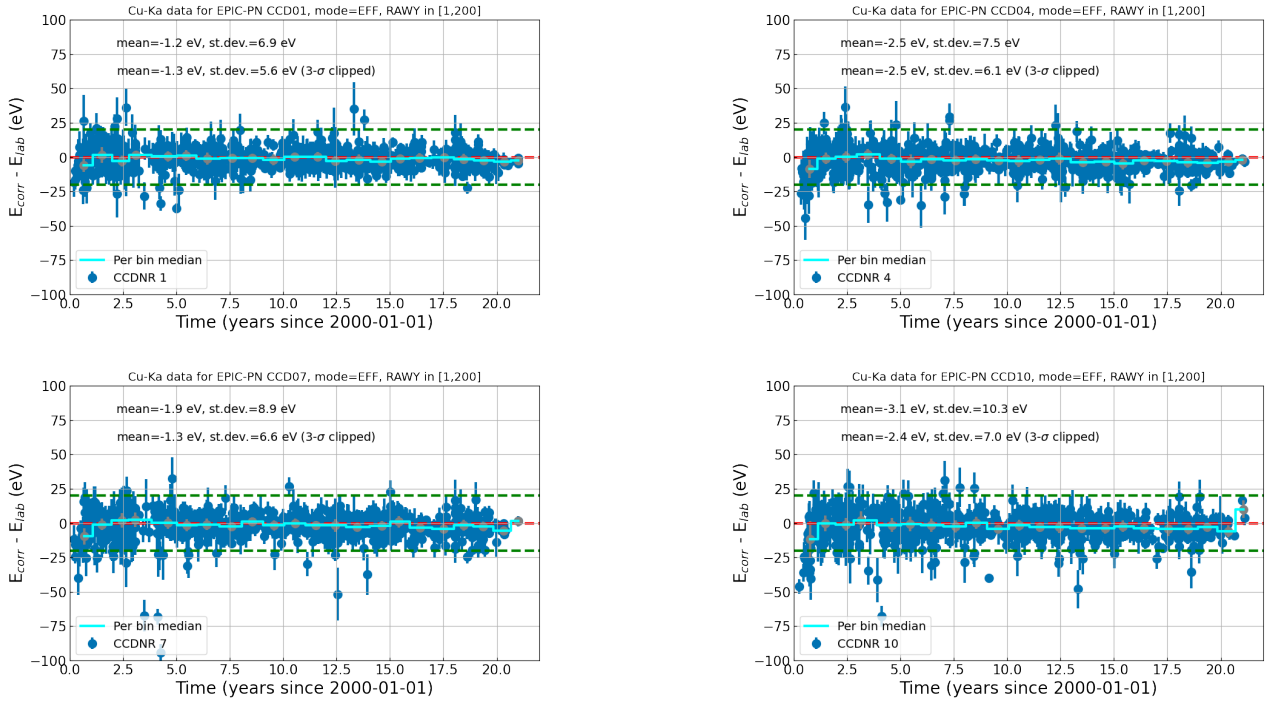

Figure 10: EFF residuals after applying the second pass LTCTI for the central CCDs. See caption of Fig. 8 for details.

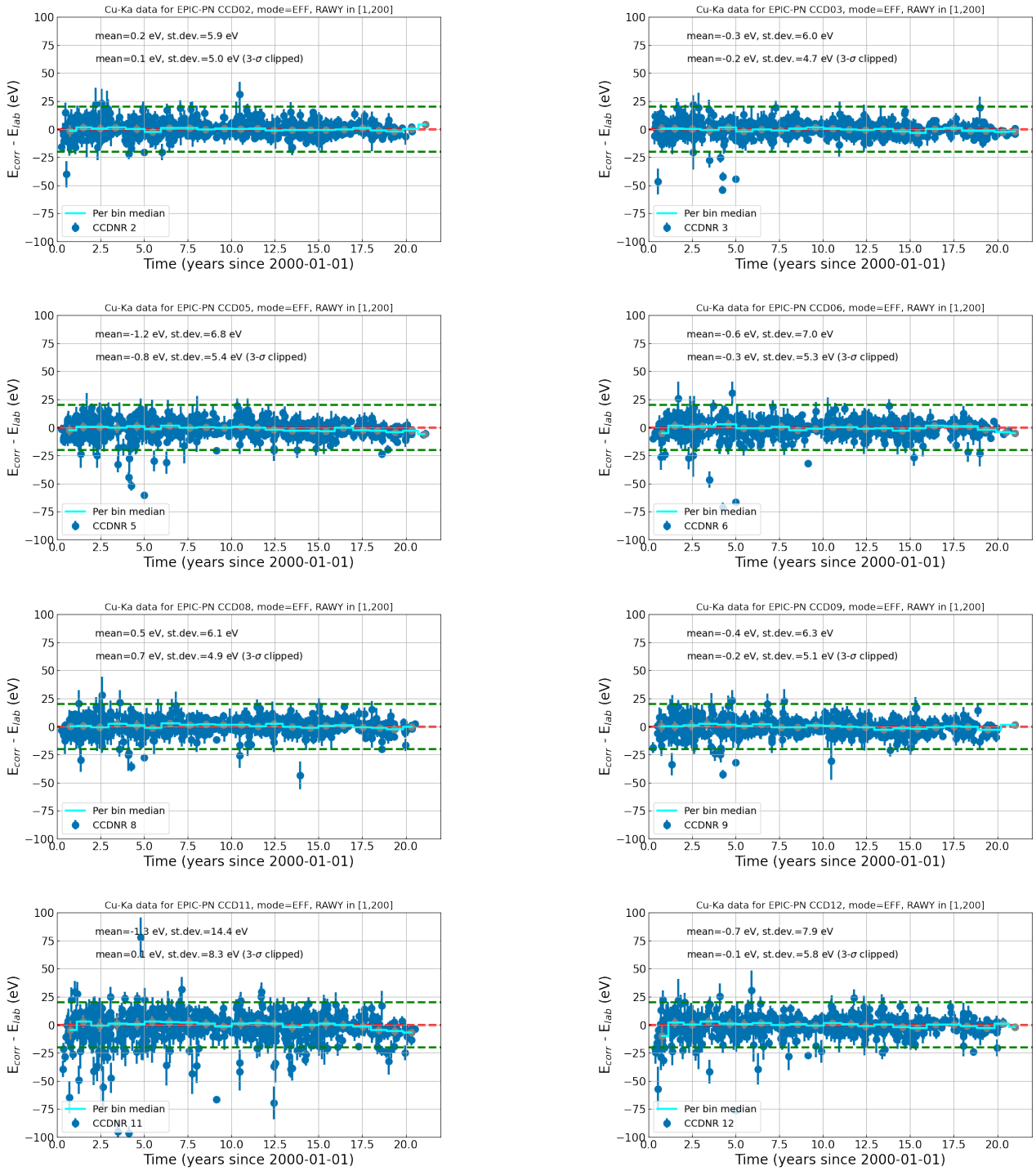

Figure 11: EFF residuals after applying the second pass LTCTI for the non-central CCDs. See caption of Fig. 8 for details.